EurJIC
European Journal of Inorganic Chemistry

Full Papers
doi.org/10.1002/ejic.202100273

Chemistry Europe
European Chemical Societies Publishing

Mono- and Di-Mesoionic Carbene-Boranes: Synthesis, Structures and Utility as Reducing Agents

Felix Stein,[a] Marius Kirsch,[a] Julia Beerhues,[a, b] Uta Albold,[a] and Biprajit Sarkar*[a, b]

Mesoionic carbenes (MIC) of the 1,2,3-triazol-5-ylidene type are currently popular ligands in organometallic chemistry. Their use in main group chemistry has been rather limited. In this contribution we present mono- and di-MIC-boranes with MICs based on triazolylidenes. The synthesis involves in-situ deprotonation of the corresponding triazolium salts and their reaction with boranes to form the desired compounds. Whereas this reaction route worked well for all triazolium salts derived from the 1,4-regioisomer of the triazoles, for the methlyene-bridged bi-triazolium salt derived from a 1,5-substiuted triazole, we observed the unexpected decomposition of the bi-triazolium and the formation of a triazole-borane with a new N–B bond. All compounds were characterized via multinuclear NMR spectroscopy, mass spectrometry, and single crystal X-ray diffraction. Furthermore, the MIC-boranes were used as reducing agents for the reduction of the C=O of aldehydes to the corresponding alcohols.

Introduction

1,2,3-Triazol-5-ylidenes, which are examples of mesoionic carbenes (MICs), have been widely used as ligands in transition metal organometallic chemistry in the last years.[1] While most of these metal complexes were tested for their activity in homogeneous catalysis, recent works have also shown the utility of such complexes in photochemistry,[2,3] in electrocatalysis,[3,4] in redox-switchable catalysis,[5] in the construction of supramolecular assemblies[6] and as electro-active compounds.[7,8] In comparison to transition metal chemistry, there are extremely few reports of the use of such MICs in combination with main-group elements.[7,9,10,11] The better σ-donor ability of these MICs in comparison to their N-heterocyclic carbene (NHC) counterparts as well as their tunable π-acceptor ability,[12] might also help in generating unusual properties with main-group elements, a fact that has already been seen often in transition metal chemistry. We have recently reported on triazoline-selones, and have used those compound to gauge the π-acceptor strength of 1,2,3-triazolylidenes.[7,12] In this report we turn our attention to the combination of 1,2,3-triazolylidenes with the element boron. More specifically, we report on the reactions of three mono-1,2,3-triazol-5-ylidenes and one bi-1,2,3-triazol-5-ylidene, all of which are derived from 1,4-disubstituted-1,2,3-triazoles, with BH_3 (Figure 1). Furthermore, we also report on the reaction of a methylene-bridged bi-1,2,3-triazol-4-ylidene, derived from a 1,5-disubstituted-1,2,3-triazole, with BH_3. The difference in the reactivities of these different isomers of triazolylidenes will be discussed. Results from multi-nuclear NMR spectroscopy, mass spectrometry, and single crystal X-ray diffraction are reported. Additionally, we show the utility of the MIC-borane adducts in the reduction of the C=O group of aldehydes to the corresponding alcohols.

Results and Discussion

Synthesis, Characterization and X-ray Crystallography

All the triazoles use in this work were reported earlier. These compounds were re-synthesized for the current work by either using the copper catalyzed azide alkyne cycloaddition (CuAAC) reaction for the 1,4-substituted triazoles (**T1**–**T4**),[13–16] or a base catalyzed azide-alkyne cycloaddition for the 1,5-substituted triazole (**T5**, see experimental section).[17] The mono triazolium salts (**L1**–**L3**, Scheme 1) were synthesized by reaction of the corresponding triazolium with CH_3I,[18] and the bitriazolium salt **L4** by the reaction of the bitriazole with Meerwein salt.[19] For the methylene-bridged bitriazolium salt **L5** a procedure,

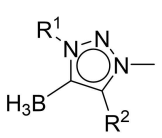

L^B1: R^1=Mes, R^2=Mes
L^B2: R^1=Dipp, R^2=Mes
L^B3: R^1=Dipp, R^2=Dipp

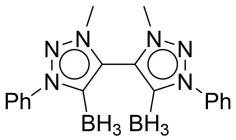

L^B4

Figure 1. Structure of Mono- and Di-Mesoionic Carbene-Boranes.

[a] F. Stein, M. Kirsch, J. Beerhues, Dr. U. Albold, Prof. Dr. B. Sarkar
Institut für Chemie und Biochemie, Freie Universität Berlin,
Fabeckstraße 34–36, 14195, Berlin, Germany
[b] J. Beerhues, Prof. Dr. B. Sarkar
Lehrstuhl für Anorganische Koordinationschemie, Institut für Anorganische Chemie, Universität Stuttgart,
Pfaffenwaldring 55, 70569, Stuttgart, Germany
E-mail: biprajit.sarkar@iac.uni-stuttgart.de
https://www.iac.uni-stuttgart.de/en/research/aksarkar/

Supporting information for this article is available on the WWW under https://doi.org/10.1002/ejic.202100273

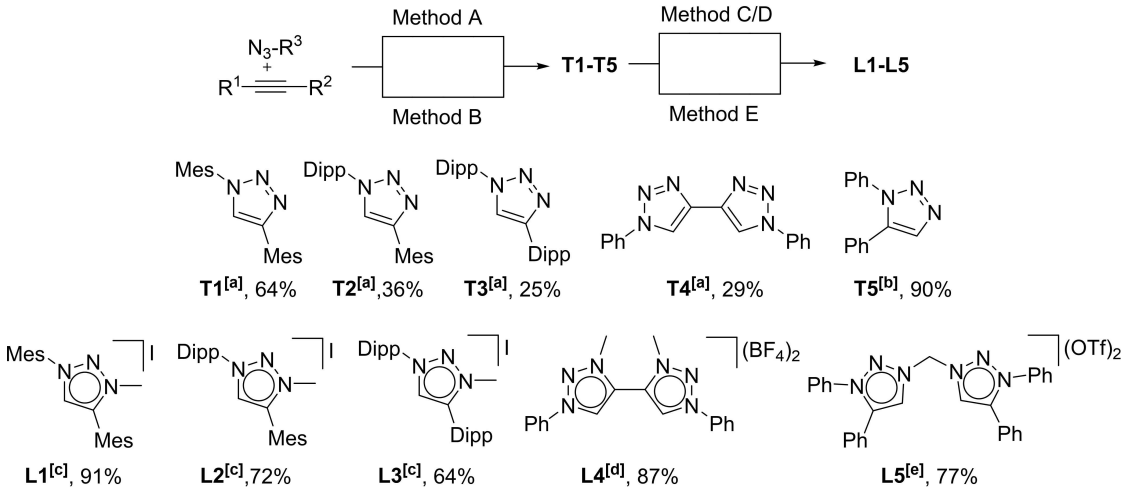

Scheme 1. Synthetic route for the synthesis of **L1**–**L5**. **Method A**[a]: $CuSO_4 \cdot 5H_2O$, sodium ascorbate, K_2CO_3, pyridine, water/t-BuOH, r.t., 3d;[13–16] **Method B**[b]: tetramethylazanium hydroxide, DMSO, r.t., 12 h;[17] **Method C**[c]: CH_3I, MeCN, 70 °C, 2d;[18] **Method D**[d]: Me_3OBF_4, DCM, r.t., 3d;[19] **Method E**[e]: Me_2I_2, AgOTf, hexane/toluene, refluxe, 12 h.[20]

recently reported by us, which is based on the preactivation of diiodomethane with AgOTf followed by a reaction with the 1,5-disubstituted triazole **T5** was used (see experimental section).[20]

The mono MIC-borane adducts **L^{B}1**–**L^{B}3** as well as the diborane aduct **L^{B}4** were all synthesized using the same procedure (Scheme 2 and experimental section). The corresponding triazolium salt was suspended in THF and cooled to 0 °C, whereupon a base was immediately added, and the mixture was stirred for 30 minutes. Afterwards BH_3·THF was slowly dropped to the reaction mixture, and the solution was allowed to warm up to room temperature overnight. The crude product was purified over a silica column (see experimental section) and the obtained compounds were characterized via ^{1}H, ^{11}B, ^{13}C NMR spectroscopy, and mass spectrometry. The moderate yield for the mono MIC-borane adducts and the low yield for the diborane adduct could be explained by the recovery of unreacted starting material. Unfortunately, prolonging of the reaction time and using more equivalents of BH_3·THF did not increase the yield in all cases. The disappearance of the signal corresponding to the C–H proton of the triazolium salt in the ^{1}H NMR spectrum of the products was a first indication of their formation (Figure S6, S9, S12, S18). In the ^{11}B spectrum a quartet was observed for all the compounds (coupling to three protons in BH_3) between −34 and −37 ppm (Figure S8, S10, S14, S19). For **L^{B}4** only one signal was observed in the ^{11}B spectrum indicating the equivalence of the two boron centers in that compound in the NMR timescale (Figure S16). The carbene-C of the compounds appeared in the ^{13}C NMR spectra between 130 and 140 ppm (Figure S7, S11, S13, S17, S20). In the ESI-MS measurements a molecular peak corresponding to the Na^+ adduct was observed for all the compounds.

The reaction of **L5** with BH_3·THF under identical conditions as described above did not lead to the desired product **L^{B}5**. Instead, a decomposition product **L^{B}6**, which is a N-coordinated triazole-borane was isolated (Scheme 3). The nucleophilicity of the N3-atom of a 1,5-substituted-1,2,3-triazole is not particularly high, and bonds between that N-atom and other groups were observed to be labile in previous works.[11] This seems to be one of the reasons for the formation of the decomposition product **L^{B}6**. In the ^{1}H NMR spectrum of this compound, a signal

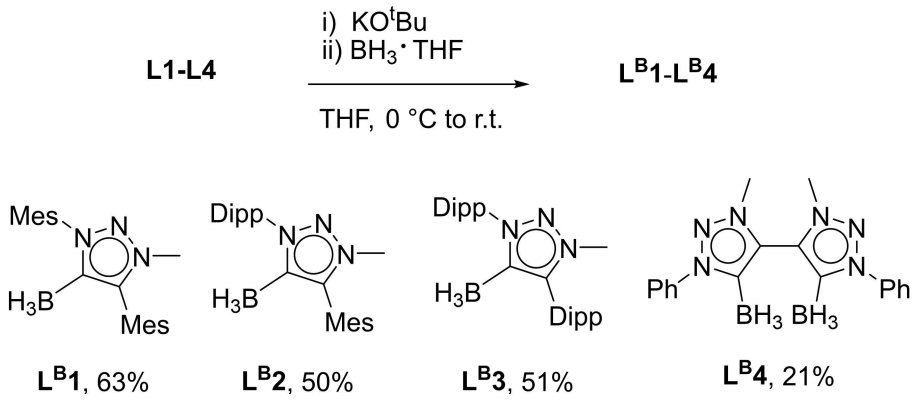

Scheme 2. Synthesis of the Mesoionic Carbene-Boranes.

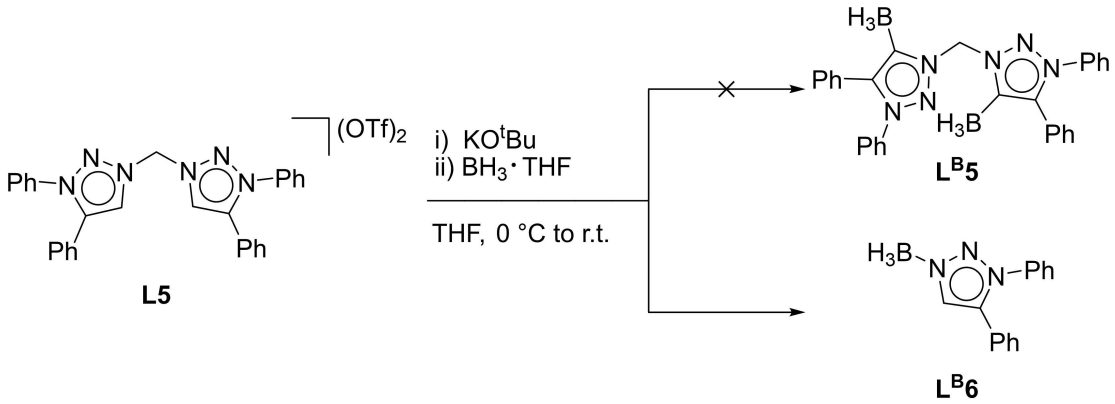

Scheme 3. Formation of **L^{B}6** by decomposition of **L^{B}5**.

corresponding to triazole C–H proton is observed at 8 ppm (Figure S18). In the ^{11}B NMR spectrum **L^{B}6** displays a broad peak at −18 ppm (Figure S19). As the boron center is now coordinated to a N-atom (instead of a C-atom as for the other compounds), the chemical shift in the ^{11}B NMR spectrum is significantly different. Additionally, the signal is broad, and the expected coupling to the three ^{1}H nuclei is not resolved. This is likely due to the quadrupolar moment of the N-atom to which the B-center is coordinated in this compound, which is known to broaden lines and preclude the observance of coupling to nuclei in the surrounding, which is otherwise expected. In the ESI-MS a molecular peak of the corresponding compound as the Na^+ adduct was observed.

The BH_3-adducts investigated in this work displayed only irreversible reduction or oxidation steps in their cyclovotammograms (Figure S21). These results point to decomposition of the compounds in response to electron transfer steps. Such an observation has been made earlier for other 1,2,3-triazol-5-ylidene type MIC adducts.[21]

We were successful in growing single crystals of **L^{B}1**, **L^{B}4** and **L^{B}6** that were suitable for X-ray diffraction measurements. The three compounds crystallize in the monoclinic $P2_1/c$, orthorhombic P_{ccn} and orthorhombic $P2_12_12_1$ crystal system and space group respectively (Table S2). The B-centers in **L^{B}1** and **L^{B}4** are coordinated to the MIC–C atom of the triazolylidene units (Figure 2). The B–C bond lengths in the two compounds are 1.600(4) and 1.607(3) Å, and are in the range of previously reported compounds. As expected, these bond lengths point to a single bond, and likely a dative nature of the C–B bond.[22] Furthermore, the N–N and C–N bond lengths within the triazolylidene rings are in the expected range (Table 1), and point to a delocalized bonding situation in the heterocyclic rings. In **L^{B}4**, there is a local inversion center in the molecule, and the rings take up an anti-orientation with respect to each other (Figure 2). The mesityl substituents in **L^{B}1** are twisted by 89.6 (1) and 70.2 (1)° with respect to the central triazolylidene ring. The two triazolylidene rings in **L^{B}4** are twisted by 55.10 (6) with respect to each other. The phenyl substituents in **L^{B}4** are twisted by 49.92 (6) and 49.92 (5)° with respect to the triazolylidene ring.

Table 1. Selected Bond Length (Å) and bond angels (°) for **L^{B}1**, **L^{B}4** and **L^{B}6**.

	L^{B}1	L^{B}4	L^{B}6
C1-B1	1.600(4)	1.607(3)	–
N3-B1	–	–	1.594(4)
N1-N2	1.320(4)	1.310(2)	1.344(3)
N2-N3	1.341(3)	1.333(2)	1.320(3)
N3-C1	1.365(4)	1.364(2)	1.347(4)
C1-C2	1.394(4)	1.387(3)	1.371(4)
C2-N1	1.463(4)	1.459(2)	1.366(4)
N1-N2-N3	102.8(2)	103.8(2)	105.2(2)

The aforementioned decomposition of **L5** and the concomitant formation of **L^{B}6** is also confirmed through the molecular structure determined in the crystal (Figure 2). The B–N bond length in this compound is 1.594(4) Å, and lies in the range of other B–N single bonds.[23] The two phenyl substituents in **L^{B}6** are twisted by 30.1 (1)° and 71.93 (9)° with respect to the central triazolylidene ring. To the best of our knowledge this is the first example of a triazole-borane adduct in which the N3-atom of a 1,2,3-triazole is coordinated to the B-atom of a borane.

Reduction of Carbonyl Functionalities

Our next step was to assess the potential of the synthesized MIC-borane adducts in the reduction of electrophilic C–O double bonds, which is shown in Table 2. To ensure good comparability, only **L^{B}1** and **L^{B}4** were tested. The protocol was selected from literature reports on similar reactions with either NHC-boranes or with MIC-boranes. All reactions were carried out in DCM at room temperature. The yield was calculated by NMR, using hexamethylbenzene as an internal standard. First, the reduction of 4-bromobenzaldehyde without the lewis acid was tested, and this led to the expected recovery of the starting material. Also, in the reaction without the MIC-borane no reduction to the alcohol was observed. Only the blank test just with BH_3·THF gave a conversion of around 30 %, which indicates the potential of boranes for the reduction of aldehydes, which was already shown previously.[24] On using $Sc(OTf)_3$ as the lewis

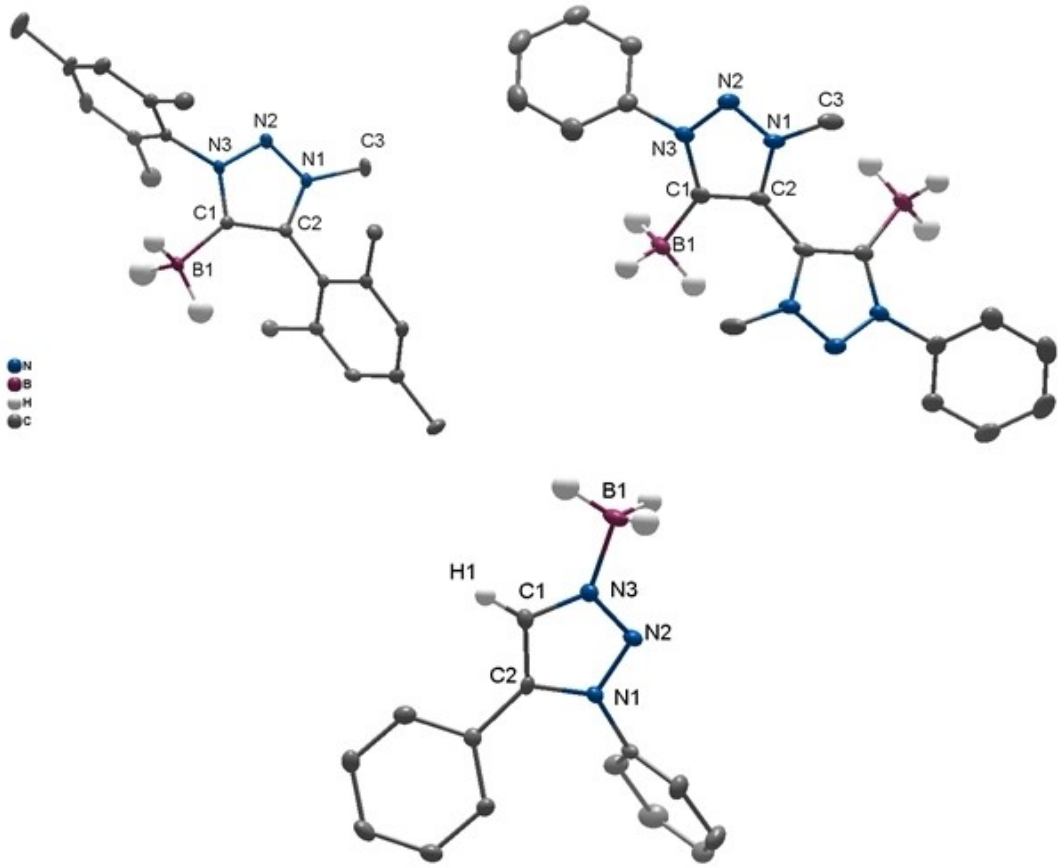

Figure 2. ORTEP representation of L^B**1**, L^B**6** and L^B**4**: ellipsoids drawn at 50% probability. Solvent molecules and H atoms omitted (except for the C–H of the triazole ring in L^B**6**) for clarity.

Table 2. Results of the reduction of different aldehydes with different MIC-BH_3-adducts as the catalyst, promoted by a lewis acid (LA).

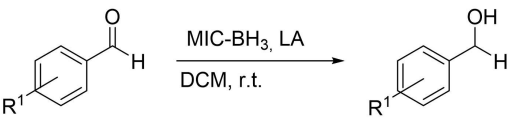

Entry	MIC-BH_3	R^1	Lewis Acid (LA)	Time [min]	Yield[a] [%]
1	–	*p*-Br	SiO_2	180	0
2	BH_3·THF	*p*-Br	SiO_2	180	35
3	L^B1	*p*-Br	–	180	0
4	L^B1	*p*-Br	20 mol% $Sc(OTf)_3$	180	71
5	L^B1	*p*-Br	SiO_2	150	99
6	L^B4	*p*-Br	–	180	0
7	L^B4	*p*-Br	20 mol% $Sc(OTf)_3$	180	12
8	L^B4	*p*-Br	SiO_2	100	99
9	L^B4	*o*-Br_2	SiO_2	60	99
10	L^B4	*p*-F	SiO_2	180	50
11	L^B4	*p*-Cl	SiO_2	180	80
12	L^B4	*p*-I	SiO_2	180	90
13	L^B4	F_5	SiO_2	180	35
14	L^B4	H	SiO_2	180	0

[a] Yield calculated by NMR using hexamethylbenzene as internal standard.

acid in combination with the MIC-boranes presented here, high conversion to the desired alcohol could be achieved with L^B**1** and low conversion with L^B**4**. By changing the additive from $Sc(OTf)_3$ to silica gel, almost quantitative conversion after 2.5 hours could be observed for both MIC-BH_3 adducts. The comparison of the reaction time of L^B**1** and L^B**4** (150 min vs. 100 min) shows the increased reduction potential of L^B**4** with the second BH_3 unit. While it is not totally clear at this moment as to why the activity of L^B**4** is higher than L^B**1**, it is likely that the presence of two BH3 units within the same molecule is beneficial for the observed reactivity. The conversion profile of the aldehyde to the alcohol for both MIC-boranes is shown in Figure 3.

We next examined the influence of the substitution pattern of the phenyl ring of the substrate on the reaction rate, using the more reactive L^B**4** as the reducing agent. By exchanging the *p*-Br with two Br in the *ortho* position, the reaction time is decreased by 1.66 times (entry 9, Table 2), which proves, that the additional steric hindrance in that substitution pattern does not hamper the reaction progress. Interestingly, exchange of the Br substituent with higher or lower homologes of the halides, the reaction progress after 180 minutes is decreased (entry 11–14). Especially, for the fluoro substituent (entry 10, Table 2), the yield goes down to 50%. In keeping with this trend, the reaction with the perfluorinated phenyl ring has the lowest yield with 35%. The enormous influence of the substitution of the phenyl ring on the outcome of the reaction

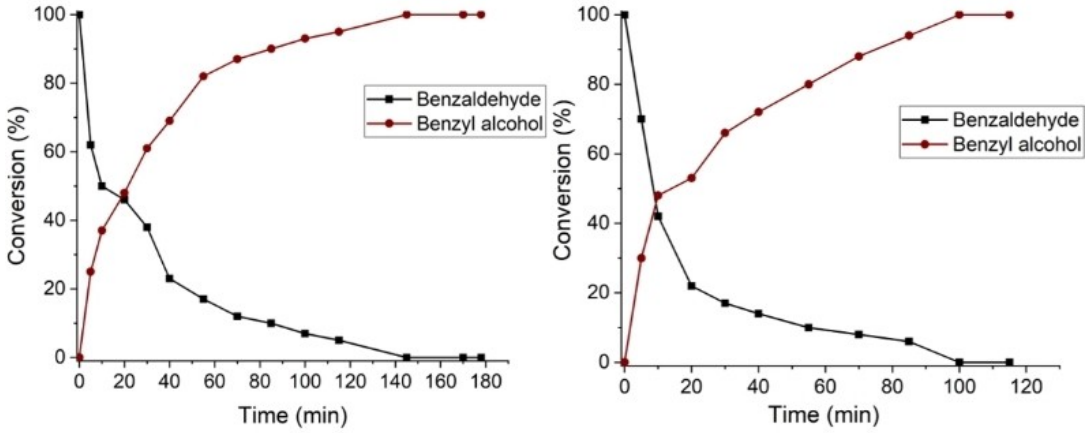

Figure 3. Percentage conversion of benzaldehyde to benzyl alcohol in DCM at r.t. Yield was calculated by NMR, using hexamethylbenzene as an internal standard. Left: L^B**1** as the catalyst; right: L^B**4** as the catalyst.

is also illustrated by the fact that simply replacing the halide in the para position with a hydrogen does not deliver any conversion after 180 min (entry 14, Table 2). Overall, the results of the reducing capacity of L^B**1** and L^B**4** are comparable with similar NHC[25] -and MIC-borane[9] systems. Especially, the diborane adduct could show higher conversion in a shorter time period, with a variety of different aldehydes.

Conclusions

In summary, we have presented here the reactions of several triazolium salts with BH_3·THF in the presence of a base. For mono-triazolium salts and the bi-triazolium salts derived from the 1,4-substituted triazoles, the reactions led to the desired formation of the mono- and the bi-MIC-borane adducts. This is the first example of a bi-MIC-bi-borane adduct based on MICs of the 1,2,3-triazol-5-ylidene type. Additionally, while reacting a methylene-bridged bi-triazolium salt with BH_3·THF under identical conditions, we have observed the formation of a new N-borane coordinated 1,2,3-triazole ring through decomposition of the bi-triazolium salt. To the best of our knowledge, this is the first example of a N3-coordinated triazole-borane adduct. All the compounds were characterized via a combination of multinuclear NMR spectroscopy, mass spectrometry and single crystal X-ray diffraction studies. Furthermore, the synthesized MIC-borane adducts were employed for reduction of halide substituted benzaldehydes, and we observed that the reaction outcome is dependent on the substitution pattern and on the reducing agent that was employed. We could also show that the reaction rate of L^B**4** is 1.5 times faster than the monosubstituted L^B**1**. Our results thus expand the main group chemistry of both triazoles and triazolylidenes, and we have also displayed the utility of the MIC-borane adducts in reduction reactions.

Experimental Section

Unless otherwise noted, all reactions were carried out using standard Schlenk-line techniques under an inert atmosphere of argon (Linde, HiQ Argon 5.0, purity $\geq$ 99.999 %). Commercially available chemicals were used without further purification. **T1**–**T3**,[13–15] **T4**[16] and **T5**[17] were prepared according to a literature known procedure. THF and diethyl ether were dried and distilled from sodium/benzophenone. Other solvents were available from MBRAUN MB-SPS-800 solvent system. For the synthesis part, all solvents were degassed by standard techniques prior to use. For NMR, $CDCl_3$ was passed through a small plug basic alumina.^{1}H NMR and ^{13}C{1H} spectra were recorded on JEOL ECS 400 spectrometer and JEOL ECZ 400R spectrometer at room temperature. Kinetic NMR spectra were recorded in Fourier transform mode with a Bruker AVANCE 500 spectrometer at 298 K. Chemical shifts are reported in ppm (relative to the TMS signal) with reference to the residual solvent peaks.[26] Multiplets are reported as follows: singlet (s), doublet (d),triplet (t) quartet (q), quintet (quint), and combinations thereof. Mass spectrometry was performed on an Agilent6210 ESI-TOF.

X-ray data were collected on a Bruker D8 Venture system at 100(2) K, using graphite-monochromated MoKα radiation ($\lambda_\alpha = 0.71073$ Å). The strategy for the data collection was evaluated by using the APEX3 software. The data were collected by $\omega + \phi$scan techniques, and were scaled and reduced using Saint+ and SADABS software. The structures were solved by intrinsic phasing methods using SHELXT-2014/7. The structure was refined by full matrix least-squares usingSHELXL-2014/7, refining on F2. Non-hydrogen atoms were refined anisotropically.[27] The contribution of disordered solvent molecules to the diffraction pattern was subtracted from the observed data by the "SQUEEZE" method as implemented in PLATON.[28]

Cyclic voltammograms were recorded with a PAR VersaStat 4 potentiostat (Ametek) by working in anhydrous and degassed MeCN (99.8 % extra dry, Acros Organics) with 0.1 M NBu_4PF_6 (dried, > 99.0 %, electrochemical grade, Fluka) as electrolyte. Concentrations of the compounds were about 1×10^{-4} M. A three-electrode setup was used with a glassy carbon working electrode, a coiled platinum wire as counter electrode, and a coiled silver wire as a pseudo-reference electrode. The ferrocene/ferrocenium couple was used as internal reference.

General procedure for the synthesis of the triazolium salts: The desired triazol and a methylating agent were dissolved in the solvent and stirred for 3 d. The reaction mixture was poured into diethyl ether and dried in vacuo, affording essentially pure triazolium salt.

Compound [L1]: T1 (700 mg, 2.29 mmol, 1 eq.), methyliodide (1.4 ml, 22.9 mmol, 10 eq.) were dissolved in MeCN (5 mL) and stirred at 70 °C. After purification by precipitation in diethylether (200 mL), the ligand was obtained as a white solid (929 mg, 2.08 mmol, 91 %).^{1}H NMR (400 MHz, $CDCl_3$): δ = 9.39 (s, 1H, triazol-H), 7.09 (m, 2H, aryl-H), 7.07 (m, 2H, aryl-H), 4.26 (s, 3H, N- CH_3), 2.39 (s, 3H, CH_3), 2.37 (s, 3H, CH_3), 2.21 (s, 6H, CH_3), 2.20 (s, 6H, CH_3) ppm.

Compound [L2]: T2 (175 mg, 0.505 mmol, 1 eq.), methyl iodide (0.3 ml, 5.05 mmol, 10 eq.) were dissolved in MeCN (4 mL) and stirred at 70 °C. After purification by precipitation in diethylether (200 mL), the ligand was obtained as a white solid (180 mg, 0.368 mmol, 72 %).^{1}H NMR (400 MHz, $CDCl_3$): δ = 9.16 (s, 1H, triazol-H), 7.65 (t, *J* = 7.9 Hz, 1H, aryl-H), 7.41(m, 2H, aryl-H), 7.09 (s, 2H, aryl-H), 4.37 (s, 3H, N-CH_3), 2.38 (s, 3H, CH_3), 2.36 (hept, *J* = 7.0 Hz, 2H, CH), 2.23 (s, 6H, CH_3), 1.27 (d, *J* = 5 Hz, 12H, CH_3) ppm.

Compound [L3]: T3 (784 mg, 2.02 mmol, 1 eq.) and methyl iodide (0.12 ml, 20.02 mmol, 10 eq.) were dissolved in MeCN (4 mL) and stirred at 70 °C. After purification by precipitation in diethylether (200 mL), the ligand was obtained as a white solid (704 mg, 1.30 mmol, 64 %). ^{1}H NMR (400 MHz, $CDCl_3$): δ = 9.29 (s, 1H, triazol-H), 7.64z (t, *J* = 7.6 Hz, 2H, aryl-H), 7.41(t, *J* = 7.4 Hz, 4H, aryl-H), 4.39 (s, 3H, N-CH_3), 2.38 (hept, *J* = 2.4 Hz, 4H, CH), 1.27 (d, *J* = 5 Hz, 12H, CH_3), 1.22 (d, *J* = 5 Hz, 12H, CH_3) ppm.

Compound [L4]: T4 (268 mg, 0.93 mmol, 1 eq.) and trimethyloxonium tetrafluoroborat (344 mg, 2.32 mmol, 2.5 eq.) were dissolved in DCM (12 ml) and stirred at room temperature. The reaction mixture was poured into diethyl ether (300 mL) and dried in vacuo, affording essentially pure ligand as a white solid (393 mg, 0.82 mmol, 87 %).^{1}H NMR (400 MHz, $(CD_3)_2CO$): δ = 10.11 (s, 2H, triazole-H), 8.02 (m, 4H, aryl-H), 7.75 (m, 6H, aryl-H), 4.5 (s, 6H, N-CH_3) ppm.

Compound [L5]: Silver triflate (1.39 g, 5.5 mmol, 2.2 eq.) was suspended in hexane (10 mL). After adding of freshly distilled diiodomethane (0.2 mL, 2.5 mmol, 1 eq.), the mixture was heated to 70 °C and stirred for 4 h under exclusion of light. The corresponding suspension with the participating silver iodide was filtered over a plug of Celite@ and washed with hexane (10 mL). The filtrate was added dropwise to **T5** (1.39 g, 6.25 mmol, 2.5 eq.) in toluene (15 mL). The resulting mixture was heated to refluxed overnight. After cooling down to room temperature, the solution was diluted in diethyl ether (500 mL). The resulting colourless precipitate was collected by filtration and washed with diethyl ether (50–100 mL), to obtain the product as a colourless solid (1.45 g, 1.92 mmol, 77 %).^{1}H NMR (400 MHz, $(CD_3)_2CO$): δ = 9.69 (s, 2H, triazol-H), 8.09 (s, 2H, aryl-H), 7.81(m, 4H, aryl-H), 7.74 (m, 2H, aryl-H), 7.65 (m, 4H, aryl-H), 7.56 (m, 7H, aryl-H), 7.47 (m, 3H, aryl-H) ppm.

General procedure for the synthesis of MIC-BH_3 adducts: The triazolium salt was suspended in THF and cooled to 0 °C. After addition of the base and stirring for 30 min., BH_3·THF [1 M] was dropped slowly to the suspension and then stirred overnight by slowly warming up to room temperature. The crude product was purified by column chromatography (SiO_2, DCM/MeOH = 50 : 1).

Compound[L^B1]: **L1** (44.7 mg, 0.10 mmol, 1eq), KO^{t}Bu (13.5 mg, 0.12 mmol, 1.2 eq.), THF (4 mL), BH_3·THF (0.1 mL, 0.1 mmol, 1 eq.). After purification by column chromatography, the product was obtained as a white solid (28.9 mg, 0.063 mmol, 63 %). ^{1}H NMR (400 MHz, $CDCl_3$): δ = 7.01 (s, 2H, Aryl-H), 7.00 (s, 2H, Aryl-H), 3.87 (s, 3H, N- CH_3), 2.36 (s, 3H, CH_3), 2.34 (s, 3H, CH_3), 2.08 (s, 6H, CH_3), 2.03 (s, 6H, CH_3) ppm. ^{11}B NMR (400 MHz, $CDCl_3$): δ = −37 (q, 3H, BH_3) ppm. ^{13}C{^{1}H} NMR (101 MHz, $CDCl_3$): δ = 142.3, 140.4, 140.3, 138.2, 134.6, 133.7, 129.1, 128.8, 122.7, 36.3, 21.4, 21.3, 19.9, 17.3 ppm. ESI-MS: m/z: [M + Na] + 356.2268 calc. 356.2267.

Compound[L^B2]: **L2** (51.1 mg, 0.10 mmol, 1eq), KO^{t}Bu (13.5 mg, 0.12 mmol, 1.2 eq.), THF (4 mL), BH_3·THF (0.1 mL, 0.1 mmol, 1 eq.). After purification by column chromatography, the product was obtained as a white solid (19.0 mg, 0.05 mmol, 50 %). ^{1}H NMR (400 MHz, $CDCl_3$): δ = 7.51 (t, *J* = 7.9 Hz, 1H, Aryl-H), 7.31 (d, *J* = 7.8 Hz, 2H, Aryl-H), 7.01 (s, 2H, Aryl-H), 3.87 (s, 3H, N-CH_3), 2.36 (sept, *J* = 6.9 Hz, 2H, CH), 2.35 (s, 3H, CH_3), 2.09 (s, 6H, CH_3), 1.29 (d, J = 6.9 Hz, 6H, CH_3), 1.13 (d, *J* = 6.9 Hz, 6H, CH_3) ppm. ^{11}B NMR (400 MHz, $CDCl_3$): δ = −36.5 (q, 3H, BH_3) ppm. ^{13}C{^{1}H} NMR (101 MHz, $CDCl_3$): δ = 145.3, 142.3, 140.4, 138.3, 133.6, 130.9, 128.8, 124.7, 123.9, 122.7, 36.3, 28.1, 24.6, 22.9, 21.4, 19.8 ppm. ESI-MS: m/z: $[M + Na]^+$ 398.2721 calc. 398.2738.

Compound[L^B3]: **L3** (26.5 mg, 0.05 mmol, 1eq), KO^{t}Bu (6.75 mg, 0.06 mmol, 1.2 eq.), THF (3 mL), BH_3·THF (0.05 mL, 0.05 mmol, 1 eq.). After purification by column chromatography, the product was obtained as a white solid (14.03 mg, 0.025 mmol, 51 %).

^{1}H NMR (400 MHz, $CDCl_3$): δ = 7.51 (m, 2H, Aryl-H), 7.32 (m, 4H, Aryl-H), 3.86 (s, 3H, N- CH_3), 2.47 (sept, *J* = 6.7 Hz, 2H, CH), 2.37 (sept, *J* = 6.7 Hz, 2H, CH), 1.30 (d, *J* = 7.0 Hz, 6H, CH_3), 1.26 (d, *J* = 7.0 Hz, 6H, CH_3), 1.19 (d, *J* = 7.0 Hz, 6H, CH_3), 1.14 (d, *J* = 7.0 Hz, 6H, CH_3) ppm. ^{11}B NMR (400 MHz, $CDCl_3$): δ = −36 (q, 3H, BH_3) ppm. ^{13}C{^{1}H} NMR (101 MHz, $CDCl_3$): δ = 149.1, 145.2, 131.2, 131.1, 123.9, 123.5, 36.6, 31.7, 29.0, 24.5, 24.2, 23.7, 22.9 ppm. ESI-MS: m/z: $[M + Na]^+$ 440.3182 calc. 440.3207.

Compound[L^B4]: **L4** (148.2 mg, 0.3 mmol, 1eq), KO^{t}Bu (80.8 mg, 0.72 mmol, 2.4 eq.), THF (10 mL), BH_3·THF (0.6 mL, 0.6 mmol, 2 eq.). After purification by column chromatography, the product was obtained as a white solid (21.8 mg, 0.063 mmol, 21 %). ^{1}H NMR (400 MHz, $CDCl_3$): δ = 7.98 (m, 4H, Aryl-H), 7.11 (m, 6H, Aryl-H), 4.33 (s, 6H, N-CH_3) ppm. ^{11}B NMR (400 MHz, $CDCl_3$): δ = −34.5 (q, 3H, BH_3) ppm. ^{13}C{^{1}H} NMR (101 MHz, $CDCl_3$): δ = 137.7, 130.8, 129.5, 125.3, 100.6, 39.5 ppm. ESI-MS: m/z: $[M + Na]^+$ 367.1982 calc. 367.1984.

Compound[L^B5]: **L5** (75.4 mg, 0.1 mmol, 1eq), KO^{t}Bu (27.0 mg, 0.22 mmol, 2.2 eq.), THF (5 mL), BH_3·THF (0.22 mL, 0.22 mmol, 2.2 eq.). After purification by column chromatography, the product could not be isolated, according to ^{1}H NMR spectroscopy, instead **L^B6** was isolated.

Compound[L^B6]: L^B6 was isolated during the attempted synthesis of **L^B5**.

^{1}H NMR (400 MHz, $CDCl_3$): δ = 8.00 (s, 1H, triazol-H), 7.52 (m,1H, aryl-H), 7.46 (m, 3H, aryl-H), 7.37 (m, 4H, aryl-H), 7.19 (m, 2H, aryl-H) ppm. ^{11}B NMR (400 MHz, $CDCl_3$): δ = −17.7 (bs, 3H, BH_3) ppm. ^{13}C{^{1}H} NMR (101 MHz, $CDCl_3$): δ = 139.9, 135.1, 131.9, 130.9, 130.8, 129.9, 129.5, 128.9, 125.4, 124.2 ppm. ESI-MS: m/z: $[M + Na]^+$ 274.0915 calc. 274.0912.

Deposition Numbers 2062463 (**L^B1**), 2062459 (**L^B4**), and 2062461 (**L^B6**) contain the supplementary crystallographic data for this paper. These data are provided free of charge by the joint Cambridge Crystallographic Data Centre and Fachinformationszentrum Karlsruhe Access Structures service www.ccdc.cam.ac.uk/structures.

Acknowledgements

We would like to thank the Core Facility BioSupraMol, supported by the DFG, for assistance with NMR und ESI-MS measurements. Open access funding enabled and organized by Projekt DEAL.

Conflict of Interest

The authors declare no conflict of interest.

Keywords: Mesoionic carbene · Triazole · Triazolylidene · Boranes · Reduction

[1] a) J. D. Crowley, A.-L. Lee, K. J. Kilpin, *Aust. J. Chem.* **2011**, *64*, 1118; b) G. Guisado-Barrios, M. Soleilhavoup, G. Bertrand, *Acc. Chem. Res.* **2018**, *51*, 3236; c) S. A. Patil, H. M. Heras-Martinez, A. M. Lewis, S. A. Patil, A. Bugarin, *Polyhedron* **2021**, *194*, 114935; d) D. Schweinfurth, L. Hettmanczyk, L. Suntrup, B. Sarkar, *Z. Anorg. Allg. Chem.* **2017**, *643*, 554; e) Á. Vivancos, C. Segarra, M. Albrecht, *Chem. Rev.* **2018**, *118*, 9493; f) R. H. Crabtree, *Coord. Chem. Rev.* **2013**, *257*, 755.

[2] a) A. Baschieri, F. Monti, E. Matteucci, A. Mazzanti, A. Barbieri, N. Armaroli, L. Sambri, *Inorg. Chem.* **2016**, *55*, 7912; b) T. Bens, P. Boden, P. Di Martino-Fumo, J. Beerhues, U. Albold, S. Sobottka, N. I. Neuman, M. Gerhards, B. Sarkar, *Inorg. Chem.* **2020**, *59*, 15504; c) D. G. Brown, N. Sanguantrakun, B. Schulze, U. S. Schubert, C. P. Berlinguette, *J. Am. Chem. Soc.* **2012**, *134*, 12354; d) L. Cao, S. Huang, W. Liu, H. Zhao, X.-G. Xiong, J.-P. Zhang, L.-M. Fu, X. Yan, *Chemistry* **2020**, *26*, 17222; e) P. Chábera, Y. Liu, O. Prakash, E. Thyrhaug, A. E. Nahhas, A. Honarfar, S. Essén, L. A. Fredin, T. C. B. Harlang, K. S. Kjær, K. Handrup, F. Ericson, H. Tatsuno, K. Morgan, J. Schnadt, L. Häggström, T. Ericsson, A. Sobkowiak, S. Lidin, P. Huang, S Styring, J. Uhlig, J. Bendix, R. Lomoth, V. Sundström, P. Persson, K. Wärnmark *Nature* **2017**, *543*, 695; f) L. Hettmanczyk, S. J. P. Spall, S. Klenk, M. van der Meer, S. Hohloch, J. A. Weinstein, B. Sarkar, *Eur. J. Inorg. Chem.* **2017**, *2017*, 2112; g) G. Kleinhans, A. K.-W. Chan, M.-Y. Leung, D. C. Liles, M. A. Fernandes, V. W.-W. Yam, I. Fernández, D. I. Bezuidenhout, *Chemistry* **2020**, *26*, 6993; h) V. Leigh, W. Ghattas, R. Lalrempuia, H. Müller-Bunz, M. T. Pryce, M. Albrecht, *Inorg. Chem.* **2013**, *52*, 5395; i) Y. Liu, K. S. Kjaer, L. A. Fredin, P. Chábera, T. Harlang, S. E. Canton, S. Lidin, J. Zhang, R. Lomoth, K.-E. Bergquist, P. Persson, K. Wärnmark, V. Sundström, *Chemistry* **2015**, *21*, 3628; j) E. Matteucci, F. Monti, R. Mazzoni, A. Baschieri, C. Bizzarri, L. Sambri, *Inorg. Chem.* **2018**, *57*, 11673; k) A. R. Naziruddin, C.-S. Lee, W.-J. Lin, B.-J. Sun, K.-H. Chao, A. H. H. Chang, W.-S. Hwang, *Dalton Trans.* **2016**, *45*, 5848; l) B. Sarkar, L. Suntrup, *Angew. Chem. Int. Ed.* **2017**, *56*, 8938; m) B. Schulze, D. Escudero, C. Friebe, R. Siebert, H. Görls, U. Köhn, E. Altuntas, A. Baumgaertel, M. D. Hager, A. Winter, B. Dietzek, J. Popp, L. González, U. Schubert, *Chemistry* 2**011**, 17, 5494; n) J. Soellner, T. Strassner, *Chemistry* **2018**, *24*, 5584; o) L. Suntrup, F. Stein, G. Hermann, M. Kleoff, M. Kuss-Petermann, J. Klein, O. S. Wenger, J. C. Tremblay, B. Sarkar, *Inorg. Chem.* **2018**, *57*, 13973; p) M. A. Topchiy, S. A. Rzhevskiy, A. A. Ageshina, N. Y. Kirilenko, G. K. Sterligov, D. Y. Mladentsev, D. Y. Paraschuk, S. N. Osipov, M. S. Nechaev, A. F. Asachenko, *Mendeleev Commun.* **2020**, *30*, 717; q) S. K. Verma, P. Kumari, S. N. Ansari, M. O. Ansari, D. Deori, S. M. Mobin, *Dalton Trans.* **2018**, *47*, 15646; r) Á. Vivancos, D. Bautista, P. González-Herrero, *Chemistry* **2019**, *25*, 6014.

[3] L. Suntrup, F. Stein, J. Klein, A. Wilting, F. G. L. Parlane, C. M. Brown, J. Fiedler, C. P. Berlinguette, I. Siewert, B. Sarkar, *Inorg. Chem.* **2020**, *59*, 4215.

[4] M. van der Meer, E. Glais, I. Siewert, B. Sarkar, *Angew. Chem. Int. Ed.* **2015**, *54*, 13792.

[5] a) L. Hettmanczyk, S. Manck, C. Hoyer, S. Hohloch, B. Sarkar, *Chem. Commun.* **2015**, *51*, 10949; b) L. Hettmanczyk, L. Suntrup, S. Klenk, C. Hoyer, B. Sarkar, *Chemistry* **2017**, *23*, 576; c) S. Klenk, S. Rupf, L. Suntrup, M. van der Meer, B. Sarkar, *Organometallics* **2017**, *36*, 2026; d) S. Vanicek, J. Beerhues, T. Bens, V. Levchenko, K. Wurst, B. Bildstein, M. Tilset, B. Sarkar, *Organometallics* **2019**, *38*, 4383; e) S. Vanicek, M. Podewitz, J. Stubbe, D. Schulze, H. Kopacka, K. Wurst, T. Müller, P. Lippmann, S. Haslinger, H. Schottenberger, K. Liedl, I. Ott, B. Sarkar, B. Bildstein, *Chemistry* **2018**, *24*, 3742.

[6] a) R. Maity, A. Mekic, M. van der Meer, A. Verma, B. Sarkar, *Chem. Commun.* **2015**, *51*, 15106; b) R. Maity, M. van der Meer, B. Sarkar, *Dalton Trans.* **2015**, *44*, 46; c) C. Mejuto, G. Guisado-Barrios, D. Gusev, E. Peris, *Chem. Commun.* **2015**, *51*, 13914; d) C. Mejuto, B. Royo, G. Guisado-Barrios, E. Peris, *Beilstein J. Org. Chem.* **2015**, *11*, 2584; e) J. Stubbe, S. Suhr, J. Beerhues, M. Nößler, B. Sarkar, *Chem. Sci.* **2021**, *12*, 3170.

[7] J. Beerhues, M. Neubrand, S. Sobottka, N. I. Neuman, H. Aberhan, S. Chandra, B. Sarkar, *Chemistry* **2021**.

[8] a) R. Maity, M. van der Meer, B. Sarkar, *Dalton Trans.* **2015**, *44*, 46; b) L. Suntrup, S. Klenk, J. Klein, S. Sobottka, B. Sarkar, *Inorg. Chem.* **2017**, *56*, 5771.

[9] L. B. de Oliveira Freitas, P. Eisenberger, C. M. Crudden, *Organometallics* **2013**, *32*, 6635.

[10] a) M. Arrowsmith, J. Böhnke, H. Braunschweig, H. Gao, M.-A. Légaré, V. Paprocki, J. Seufert, *Chemistry* **2017**, *23*, 12210; b) M. Begtrup, *Tetrahedron Lett.* **1971**, *12*, 1577; c) M. Begtrup, C. Pedersen, B. Jerslev, A. Kallner, *Acta Chem. Scand.* **1965**, *19*, 2022; d) D. I. Bezuidenhout, G. Kleinhans, G. Guisado-Barrios, D. C. Liles, G. Ung, G. Bertrand, *Chem. Commun.* **2014**, *50*, 2431; e) K. Bouchemella, K. Fauché, B. Anak, L. Jouffret, M. Bencharif, F. Cisnetti, *New J. Chem.* **2018**, *42*, 18969; f) B.-L. Chen, Y. Zhang, Y.-R. Lei, H.-M. Wang, Z. Chen, *Chem. Commun.* **2020**, *56*, 5787; g) P. Eisenberger, B. P. Bestvater, E. C. Keske, C. M. Crudden, *Angew. Chem. Int. Ed.* **2015**, *54*, 2467; h) L. Y. M. Eymann, R. Scopelliti, F. F. Tirani, K. Severin, *Chemistry* **2018**, *24*, 7957; i) M. M. Hansmann, P. W. Antoni, H. Pesch, *Angew. Chem. Int. Ed.* **2020**, *59*, 5782; j) J. Lam, B. A. R. Günther, J. M. Farrell, P. Eisenberger, B. P. Bestvater, P. D. Newman, R. L. Melen, C. M. Crudden, D. W. Stephan, *Dalton Trans.* **2016**, *45*, 15303; k) Q. Liang, K. Hayashi, D. Song, *Organometallics* **2020**, *39*, 4115; l) Y. Liu, P. Varava, A. Fabrizio, L. Y. M. Eymann, A. G. Tskhovrebov, O. M. Planes, E. Solari, F. Fadaei-Tirani, R. Scopelliti, A. Sienkiewicz, C. Corminboeuf, K. Severin, *Chem. Sci.* **2019**, *10*, 5719; m) T. Maulbetsch, D. Kunz, *Angew. Chem. Int. Ed.* **2021**, *60*, 2007; n) L. D. M. Nicholls, M. Marx, T. Hartung, E. González-Fernández, C. Golz, M. Alcarazo, *ACS Catal.* **2018**, *8*, 6079; o) R. Nomura, Y. Tsuchiya, H. Ishikawa, S. Okamoto, *Tetrahedron Lett.* **2013**, *54*, 1360; p) A. Petronilho, H. Müller-Bunz, M. Albrecht, *Chem. Commun.* **2012**, *48*, 6499; q) M. Vaddamanu, G. Prabusankar, *Eur. J. Inorg. Chem.* **2020**, *2020*, 2403; r) M. Vaddamanu, K. Velappan, G. Prabusankar, *New J. Chem.* **2020**, *44*, 129; s) H. Wang, B. Zhang, X. Yan, S. Guo, *Dalton Trans.* **2018**, *47*, 528; t) Z. Zhang, S. Huang, L. Huang, X. Xu, H. Zhao, X. Yan, *J. Org. Chem.* **2020**, *85*, 12036.

[11] J. Stubbe, N. I. Neuman, R. McLellan, M. G. Sommer, M. Nößler, J. Beerhues, R. E. Mulvey, B. Sarkar, *Angew. Chem. Int. Ed.* **2021**, *60*, 499.

[12] J. Beerhues, H. Aberhan, T.-N. Streit, B. Sarkar, *Organometallics* **2020**, *39*, 4557.

[13] T. Nakamura, T. Terashima, K. Ogata, S.-i. Fukuzawa, *Org. Lett.* **2011**, *13*, 620.

[14] T. Nakamura, K. Ogata, S.-i. Fukuzawa, *Chem. Lett.* **2010**, *39*, 920.

[15] S. Khan, J. Liebscher, *Synthesis* **2010**, *2010*, 2609.

[16] J. T. Fletcher, B. J. Bumgarner, N. D. Engels, D. A. Skoglund, *Organometallics* **2008**, *27*, 5430.

[17] S. W. Kwok, J. R. Fotsing, R. J. Fraser, V. O. Rodionov, V. V. Fokin, *Org. Lett.* **2010**, *12*, 4217.

[18] S. Hohloch, C.-Y. Su, B. Sarkar, *Eur. J. Inorg. Chem.* **2011**, *2011*, 3067.

[19] S. Hohloch, L. Suntrup, B. Sarkar, *Organometallics* **2013**, *32*, 7376.

[20] L. Suntrup, S. Hohloch, B. Sarkar, *Chemistry* **2016**, *22*, 18009.

[21] a) L. Hettmanczyk, S. J. P. Spall, S. Klenk, M. van der Meer, S. Hohloch, J. A. Weinstein, B. Sarkar, *Eur. J. Inorg. Chem.* **2017**, *2017*, 2112; b) S. Klenk, S. Rupf, L. Suntrup, M. van der Meer, B. Sarkar, *Organometallics* **2017**, *36*, 2026.

[22] a) K. Niedenzu, J. W. Dawson, *Boron-Nitrogen Compounds*, Springer, Berlin, Heidelberg, **1965**; b) D. Prieschl, G. Bélanger-Chabot, X. Guo, M. Dietz, M. Müller, I. Krummenacher, Z. Lin, H. Braunschweig, *J. Am. Chem. Soc.* **2020**, *142*, 1065.

[23] a) I. I. Padilla-Martnez, N. Andrade-Lpez, M. Gama-Goicochea, E. Aguilar-Cruz, A. Cruz, R. Contreras, H. Tlahuext, *Heteroat. Chem.* **1996**, *7*, 323; b) C. F. Pupim, A. J. L. Catão, A. López-Castillo, *J. Mol. Model.* **2018**, *24*, 283; c) N. Schulenberg, M. Jäkel, E. Kaifer, H.-J. Himmel, *Eur. J. Inorg. Chem.* **2009**, *2009*, 4809; d) A. Wacker, C. G. Yan, G. Kaltenpoth, A. Ginsberg, A. M. Arif, R. D. Ernst, H. Pritzkow, W. Siebert, *J. Org. Chem.* **2002**, *641*, 195.

[24] N. M. Yoon, C. S. Pak, B. H. C. S. Krishnamurthy, T. P. Stocky, *J. Org. Chem.* **1973**, *38*, 2786.

[25] T. Taniguchi, D. P. Curran, *Org. Lett.* **2012**, *14*, 4540.

[26] G. R. Fulmer, A. J. M. Miller, N. H. Sherden, H. E. Gottlieb, A. Nudelman, B. M. Stoltz, J. E. Bercaw, K. I. Goldberg, *Organometallics* **2010**, *29*, 2176.
[27] a) *APEX3*, Bruker AXS Inc., Madison, Wisconsin, USA, **2015**; b) G. M. Sheldrick, *SADABS Ver. 2008/1, Program for Empirical Absorption Correction*, University of Göttingen, Germany, **2008**; c) *SAINT+, Data Integration Engine, Version 8.27b* ©, Bruker AXS Inc., Madison, Wisconsin, USA, **1997–2012**; d) G. M. Sheldrick, *SHELXL Version 2014/7, Program for Chrystal Structure Solution and Refinement*, University of Göttingen, Germany, 2014; e) C. B. Hübschle, G. M. Sheldrick, B. Dittrich, *J. Appl. Crystallogr.* **2011**, *44*, 1281; f) G. M. Sheldrick, *Acta Crystallogr.* **2008**, *A64*, 112; g) G. M. Sheldrick, *Acta Crystallogr.* **2015**, *C71*, 3.17; h) A. L. Spek, *Acta Crystallogr.* **2015**, *C71*, 9; i) A. L. Spek, *ActaCryst.* **2009**, *D65*, 148; j) A. L. Spek, *J. Appl. Crystallogr.* **2003**, *36*, 7.
[28] a) A. L. Spek, *PLATON, A multipurpose Crystallographic Tool*, Utrecht, the Netherlands, **1998**; b) A. L. Spek, *ActaCryst.* **2009**, *D65*, 148; c) A. L. Spek, *J. Appl. Crystallogr.* **2003**, *36*, 7.

Manuscript received: April 6, 2021
Revised manuscript received: May 1, 2021
Accepted manuscript online: May 12, 2021